JOURNAL OF THERMOPHYSICS AND HEAT TRANSFER
Vol. 13, No. 1, January–March 1999

Interfacial Contact Resistance of Single-Crystal Ceramics for Solar Concentrators

S. R. Mirmira* and L. S. Fletcher†
Texas A&M University, College Station, Texas 77843-3123
and
K. W. Baker‡
NASA Lewis Research Center, Cleveland, Ohio 44135

An experimental investigation was conducted to determine the thermal conductivity and overall thermal resistance of stacks of single-crystal alumina and magnesia, and zirconia. From these data, the interfacial thermal resistance between the ceramic materials was evaluated over a range of pressures of 70–1720 kPa, and at two temperatures of 20 and 60°C. For all three materials, the interfacial thermal resistance decreases significantly with an increase in pressure at lower pressures, beyond which it decreases more gradually. Further, the effect of temperature on the interfacial thermal resistance is negligible for the temperature range investigated. These data were used to develop an equation relating the dimensionless interfacial thermal resistance to the crystal material properties, surface characteristics, crystal thickness, apparent interface pressure, and mean interface temperature.

Nomenclature

D_q = asperity slope
F = flatness of crystals
H = microhardness of ceramic crystals
k = thermal conductivity of crystals
P = pressure
R = roughness of crystals
R_c = contact resistance
T = absolute temperature
t = thickness of each ceramic crystal
W = waviness of crystals
β = coefficient of linear expansion

Subscripts
a = average
q = root mean square
v = Vickers

Introduction

OVER the last decade, the world has seen rapid advances in space-related technology. As a direct consequence of these advancements, the large-scale harnessing of solar energy in outer space may soon be a reality. As the potential has developed for withstanding extremely high temperatures (2500 K) in solar heat receivers, it has become necessary to utilize primary and secondary concentrators to harness this large amount of energy. Secondary concentrators refocus the already concentrated solar energy from the primary collector, thereby reducing the light entrance aperture and the associated radiation losses. Further, secondary concentrators increase the focusing accuracy required to achieve high concentration ratios. Presently, engineers are in the process of assessing the feasibility of high refractive index materials in the manufacture of these secondary concentrators.

The use of high refractive index materials for solar concentrators rather than hollow reflective materials has several advantages, including easier fabrication, higher thermal efficiency (~95% rather than ~80%), and there are no special cooling requirements. There also exist several technical challenges in the design and fabrication of secondary concentrators, including the selection of a suitable optical material capable of withstanding high temperatures. Prime candidates are single-crystal optically clear sapphire or aluminum oxide, magnesium oxide, and zirconium oxide. It is planned to design and fabricate the secondary concentrator by arranging single crystals of the same material in a multilayer stack. Consequently, knowledge of the thermal conductivity and interfacial thermal resistance of these materials is extremely critical for the proper design of concentrators.

Multilayer stacks of ceramic materials are capable of providing effective thermal insulation as a result of high interfacial resistance.[1] This high thermal resistance may be attributed to the low ratio of actual to apparent contact area caused by microscopic irregularities that cause the heat flow to be constricted.[2,3] The relatively low thermal conductivity and high hardness of these materials also tends to increase the thermal resistance at each interface. Furthermore, theoretical predictions of thermal resistance for multilayer stacks of materials are more complex than those for single interfaces.[4] In the latter case, deformation mechanisms are dictated by the mechanical properties of the substrate, while the stack deformation can vary from layer flattening for thin samples at low loads to asperity deformation at high loads.[5]

The thermal contact conductance of coatings of aluminum, copper, iron carbide, and aluminum plus copper on alumina substrates in contact with aluminum 6061 was experimentally determined by Chung et al.[6] The aluminum oxide coated with aluminum plus copper had the highest contact conductance values that increased with an increase in pressure. The authors also examined the effect of surface roughness on thermal contact conductance. In this case as well, the aluminum plus copper coating showed the greatest improvement.

Fletcher and Sparks[7] conducted an experimental study to determine the effective thermal conductivity and thermal contact conductance of selected porous ceramic materials, includ-

Presented as Paper 98-0894 at the AIAA 36th Aerospace Sciences Meeting, Reno, NV, Jan. 12–15, 1998; received Feb. 2, 1998; revision received Aug. 26, 1998; accepted for publication Sept. 15, 1998.

*Graduate Research Assistant, Mechanical Engineering Department. Student Member AIAA.
†Thomas A. Dietz Professor, Mechanical Engineering Department. Fellow AIAA.
‡Research Scientist.

Table 1 Characteristic properties of selected ceramic materials

Material	Dimensions, mm	Thermal conductivity, W/mK[13]	Melting point, K	Linear expansion, 10^{-6}/K	Index of refraction	Microhardness, H_v
Alumina	25.4 mm disk	47 @ 300 K	——	——	——	——
	3.43 mm thick	10 @ 1000 K	~2305	7.2–8.6	1.76	~1050
	——	6 @ 2500 K	——	——	——	——
Magnesia	15 mm square	60 @ 300 K	——	——	——	——
	3.35 mm thick	8 @ 1500 K	~3071	12.3–16.0	1.76	~685
Zirconia, 8 mole % *Y*	25.4 mm disk	——	——	——	——	——
	6.61 mm thick	1.3 @ 400 K	~2980	10.5	2.16	~1320

ing aluminum oxide, partially stabilized zirconia, and mullite-bonded silicon carbide. The paper reports that the overall thermal conductance increased with increasing temperature and porosity. Based on the fact that the thermal characteristics for these ceramic materials are similar, the authors conclude that the applications of these porous ceramics are governed more by the mechanical properties than their thermal characteristics.

Thomas and Probert[8] and Al-Astrabadi et al.[9] determined the contact conductance of stacks of thin metallic layers. Results obtained by Al-Astrabadi et al.[9] indicate two distinct modes of compression, a layer-flattening region at low loads and a surface waviness deformation region at higher loads. Further, hystereses in thermal resistance and compression characteristics were observed during the initial loading/unloading cycle.

Al-Astrabadi et al.[10] also measured the thermal resistance of thin (<3.5 mm) Melinex, Perspex, Tufnol, polytetrafluroethylene (PTFE), and mica inserts between flat stainless-steel surfaces in the absence of any grease or lubricant. The results indicated that the presence of nonmetallic shims led to an increase of 10–1000 in the thermal resistance of the steel-to-steel joint. However, the introduction of a second layer of the same material increased the overall resistance by only 10%. Considering the fact that most bearing surfaces are dynamic and not static in nature, the authors conclude that PTFE is the most suitable insert for thermal isolation.

An experimental and theoretical study of the interfacial and overall thermal resistance of thin layers of aluminum oxide of either 1.00 or 0.65 mm in thickness, arranged in stack form, was conducted by Babus'Hag et al.[11] The total thermal resistance was measured for stacks comprising 2, 5, 15, and 30 layers of alumina, over a range of pressures. The paper reports that as the pressure increases, the thermal resistance decreased as a result of the increase in the number of microcontacts and of the surfaces conforming to their microscopic topographies. The paper concludes that the overall thermal insulation provided by a multilayer stack of alumina is proportional to the number of interfaces. The authors attribute this high mean thermal resistance value to the low ratio of actual to nominal contact area between adjacent alumina layers, high hardness of alumina, and the relatively low bulk thermal conductivity.

Based on this literature review, and also considering the wide range of applications of multilayer stacks composed of single-crystal ceramic materials, it appears that there is a lack of interfacial thermal resistance information. In addition to the limited experimental thermal resistance data for stacks of single crystals, there does not appear to be any analytical technique for predicting the interfacial thermal resistance for stacks of single crystal.

Experimental Program

To provide additional experimental data on the interfacial resistance between ceramic single-crystal samples that may be used in the design and fabrication of secondary solar concentrators, the following experimental program was undertaken.

Material Selection

Table 1 lists the selected thermophysical properties of the single-crystal ceramics considered as suitable materials for solar concentrators. This experimental study provides data for multilayer stacks of sapphire and magnesium-oxide single crystals, and yttrium- (8 mole %) stabilized zirconia. The alumina and zirconia crystals were 2.54 cm in diameter, whereas the magnesia samples were 15 mm in size. The thickness of alumina and zirconia crystals were 3.43 and 6.61 mm, respectively, whereas the magnesia crystals were 3.35 mm in thickness.

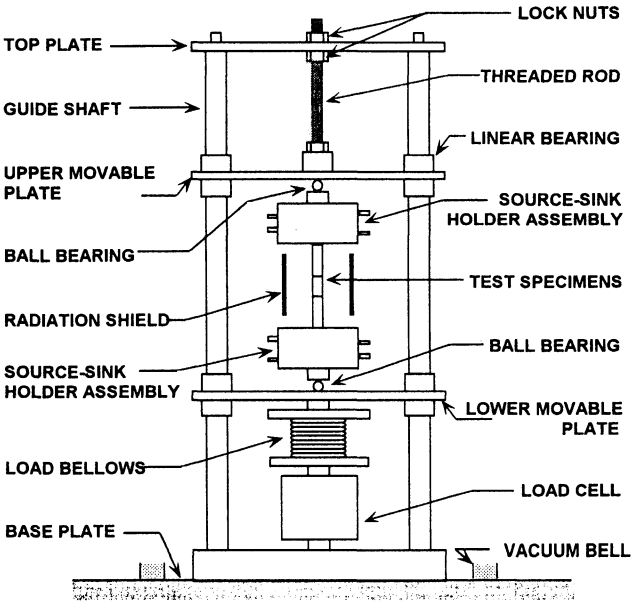

Fig. 1 Schematic representation of test facility.

Test Facility

The test facility used for this experimental investigation involved a vertical column consisting of a frame with sliding plates for support of two combination heat source/sink specimen holder assemblies, the test samples, a load cell, and pneumatic bellows, as shown in Fig. 1. An axial force was applied on the vertical column including the test specimens by pressurizing the bellows with nitrogen. The contact load was monitored by a load cell and signal amplifier. Uniform contact pressure over the contacting test interfaces was assured by the use of two hardened stainless-steel balls that transferred the load from the frame to the source-sink-holder assemblies, and in turn, to the test interface. A band heater was placed around the upper flux-meter holder to provide the heat flux. Coolant (ethylene glycol) was introduced through the lower flux-meter holder by means of flexible neoprene hoses. The use of such neoprene hoses minimizes lateral loads that may distort the pressure distribution over the interfaces. The experimental facility was housed in a vacuum environment at a pressure of 1×10^{-5} torr, which was maintained by a oil-diffusion pump backed by a two-stage rotary pump, and this vacuum pressure was monitored by thermocouple and filament gauges.

The vertical test column consisted of electrolytic iron upper and lower flux meters and the stack of crystal samples to be

tested. To account for the variable shapes of the ceramic crystal (alumina and zirconia-disks, magnesium oxide-square) samples, two vertical test configurations were used. In the case of the sapphire and zirconia disks, the diameter of the flux meters was 2.54 cm (1.00 in.), and the lengths were 10.16 cm. To determine the interfacial resistance between the MgO disks, flux meters of 1.5 cm square were used. In both cases, a stack of single crystals was placed at the interface of the two electrolytic iron heat flux meters. The flux meters were instrumented with 30-gauge, Teflon®/Teflon sheath, special limit of error type K chrome/alumel thermocouples to enable the calculation of the temperature gradient, the temperature difference across the crystal stack, and the heat flux normal to the interface.

Prior to measuring the interfacial thermal resistance, the thermal conductivity of the sapphire, zirconia, and magnesium oxide was determined over a temperature range of 0–100°C. It is these experimentally determined thermal conductivity values that were used to calculate the thermal resistance. To ensure repeatability of the thermal conductivity results, three samples of each material were tested. To minimize the contact resistance at the crystal/heat flux-meter interfaces, thermal conductivity tests were conducted at a mean interface pressure of 2067 kPa and thermal grease (Dow Corning 340-Silicone Heat Sink Compound) was applied between the sample and flux-meter surfaces.

Figure 2 shows the thermal conductivity of the alumina, magnesia, and zirconia samples used in this investigation as a function of mean interface temperature. It is apparent that the thermal conductivity of alumina and magnesia is a function of temperature, and decreases with an increase in temperature. The thermal conductivity of single-crystal sapphire ranged from 32 to 21 W/mK over the specified temperature range, whereas the values for magnesium oxide varied from 64 to 45 W/mK. On the other hand, the thermal conductivity of zirconia did not vary significantly with temperature and was also much lower in magnitude. Figure 2 also shows the thermal conductivity of these materials as obtained by other researchers. A comparison with published values[12–14] indicates that the present values show a similar trend with temperature. The thermal conductivity values obtained at 20 and 60°C were used to calculate the bulk resistance of the crystals at these temperatures.

The thermal contact resistance between contacting sapphire, magnesia, and zirconia samples arranged in stack form was evaluated at pressures ranging from 69–1725 kPa, and at interface temperatures of 20 and 60°C. Further, no thermal grease was applied at the interface between the crystals for contact conductance tests.

A surface characterization of the electrolytic iron flux meters and the alumina, magnesia, and zirconia samples was obtained prior to testing with a Federal Products Surfanalyzer 5000/400. The surface trace enabled the determination of the overall flatness deviation (F), average (R_a) and rms (R_q) roughness, waviness (W_a), and asperity slope (D_q). These surface characteristics are provided in Table 2.

The microhardness of the ceramic crystals utilized in this experimental investigation was measured using a Buehler Micromet II. The average of 10 readings obtained at room temperature for each type of crystal sample are reported in Table 1. It is noteworthy that these materials possess an extremely high microhardness value compared with metals such as aluminum.

Experimental Procedure

The electrolytic iron flux meters and the single-crystal samples were inserted carefully into the test facility and aligned. A nominal axial load was applied to the heat flux meters to ensure the surfaces remained in contact during evacuation of the chamber. The test temperatures and applied load were automatically controlled by a personal computer via an IEEE-48 bus and feedback loop through a Hewlett-Packard data acqui-

Table 2 Average surface characteristics of alumina, magnesia (single crystal), and zirconia samples

Material	F, μm	R_a, μm	R_q, μm	W_a, μm	D_q
Alumina	3.81	0.07	0.08	0.41	0.008
Magnesia	3.75	0.07	0.08	0.43	0.006
Zirconia	30.41	2.45	3.24	1.71	0.026
Electrolytic iron	10.20	0.22	0.36	0.84	0.009

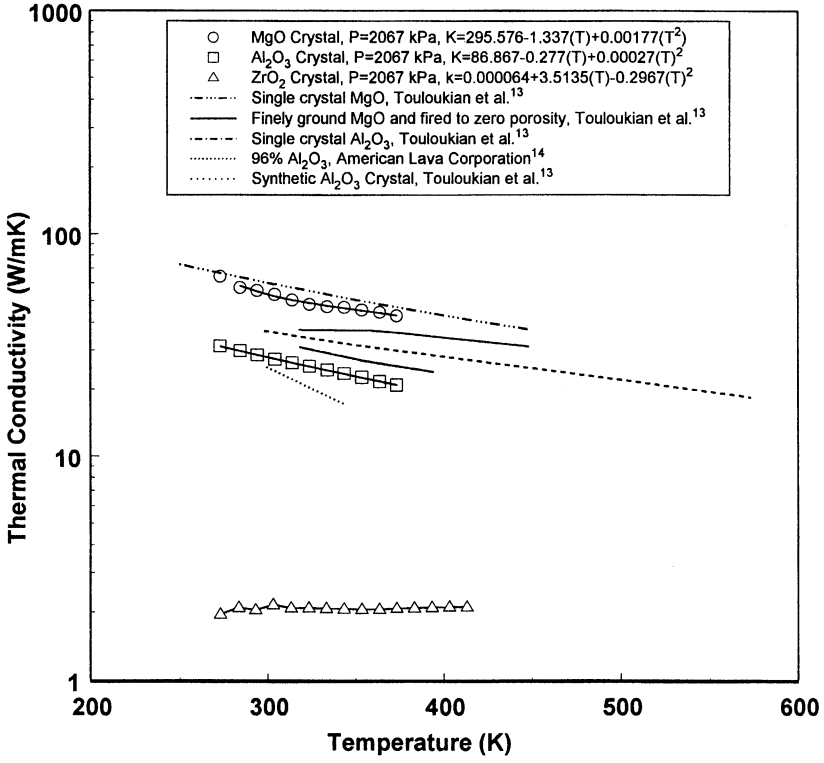

Fig. 2 Thermal conductivity of selected ceramic materials as a function of temperature.

sition system. The heat fluxes in the upper and lower flux meters as well as through the stack of crystals, were determined from the temperature gradients and thermal conductivity of the electrolytic heat flux meters. The difference in temperature across the stack of crystals was determined by extrapolating the temperature gradient in the heat flux meters to the respective crystal interface. Radiative losses from the flux meters and sample were reduced by placing a radiation shield around the vertical test column and, to avoid convection losses, the entire test facility was housed in a vacuum chamber.

The single-crystal samples were not instruments with thermocouples because of the limited thickness of the samples. The thermal contact resistance data are for the case of a heat flux passing from the upper electrolytic iron flux meter through the stack of crystals to the lower electrolytic iron flux meter.

Uncertainty Analysis

The uncertainty involved in the various parameters and quantities used to compute the thermal contact conductance can be combined to arrive at one overall relative uncertainty value. The Kline and McClintock[15] uncertainty analysis was employed to determine this overall relative uncertainty in the thermal contact conductance.

The overall uncertainty in the reported values of thermal conductivity and contact conductance of the crystal materials is composed of various parameters. These parameters include, uncertainty in thermal conductivity of the base material (electrolytic iron), the heat flux across the cross-sectional area, the temperature gradients within the iron flux meters, location tolerances for the *special limit of error* thermocouples, the temperature readings, and the temperature difference across the junction of the crystal stack employed.

The total average overall uncertainty of the thermal conductivity of each base electrolytic iron material is 1.5%. The uncertainty in the temperature reading of the special limit of error thermocouples is 1.1°C or 0.4% above 0°C. The total uncertainty of the thermal temperature gradients within the iron flux meters, location tolerance of the thermocouple holes, and the dimensional tolerance for the cross-sectional area is ~0.6%. Based on this uncertainty analysis, the average uncertainty in the effective thermal conductivity was within ±3.0%.

The average overall uncertainty in the thermal contact conductance for each stack of materials was the accumulation of the uncertainties mentioned for the thermal conductivity case with the addition for uncertainty caused by the temperature difference across the junction and the dimensional tolerance for the cross-sectional area of the sample. The overall uncertainty value in the conductance value has been determined as ±5%.

Results and Discussion

The total thermal contact resistance (bulk material resistance and interfacial resistances) between highly polished single-crystal ceramic materials (alumina and magnesia), and zirconia (yttrium stabilized) arranged in stack form was determined over a pressure range of 70–1722 kPa and at mean interface temperatures of 20 and 60°C. These thermal contact resistance data at specific mean interface temperatures are presented as a function of apparent interface pressure, and are beneficial for the selection of a material in the fabrication of secondary concentrators. Further, these data may also be used to estimate the heat/energy losses caused by the interfacial thermal resistance.

The total interfacial thermal contact resistance (the bulk resistance, t/k, has been subtracted from the total resistance) for stacks of single-crystal alumina (six samples), magnesia (five samples), and zirconia (four samples), as a function of apparent interface pressure at 20°C is shown in Fig. 3. With an increase in the applied pressure from 70–345 kPa, the total thermal resistance decreases significantly, after which it de-

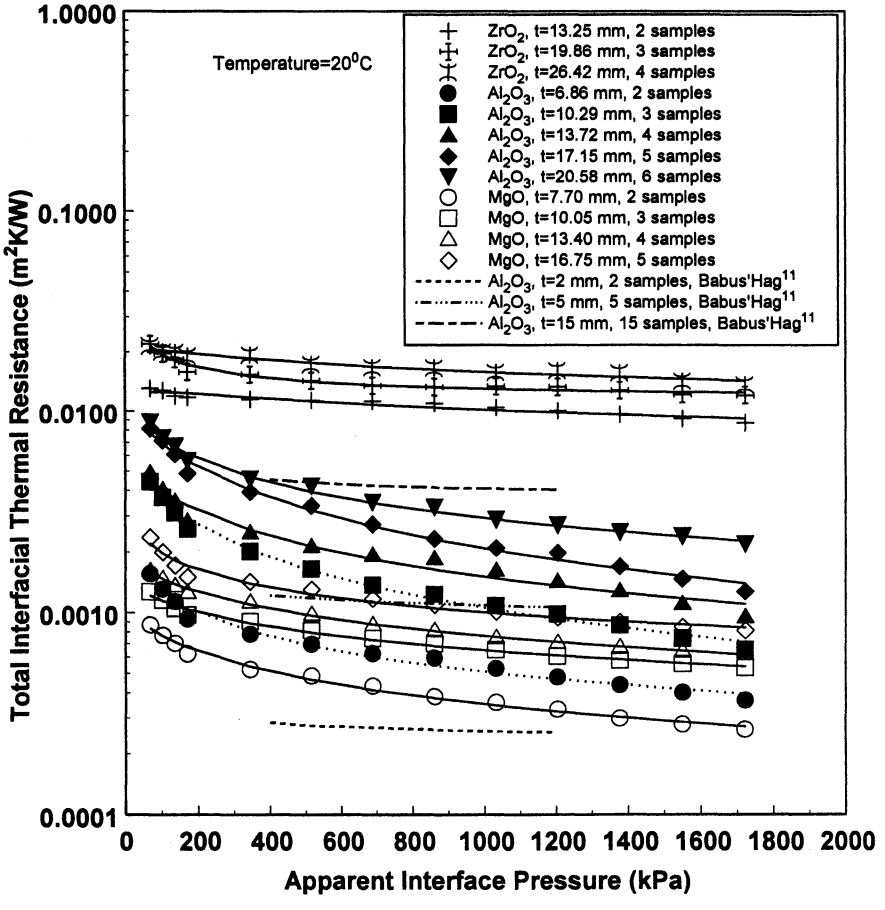

Fig. 3 Total interfacial thermal resistance of interfaces between alumina, magnesia (single crystal), and yttrium-stabilized zirconia at 20°C.

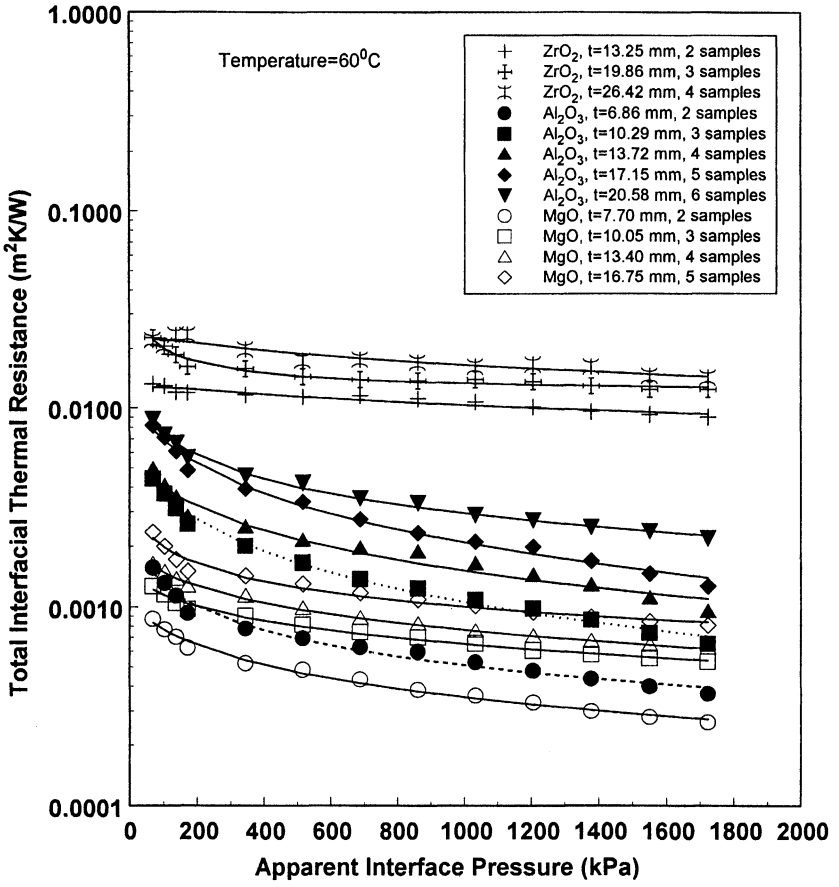

Fig. 4 Total interfacial thermal resistance of interfaces between alumina, magnesia (single crystal), and yttrium-stabilized zirconia at 60°C.

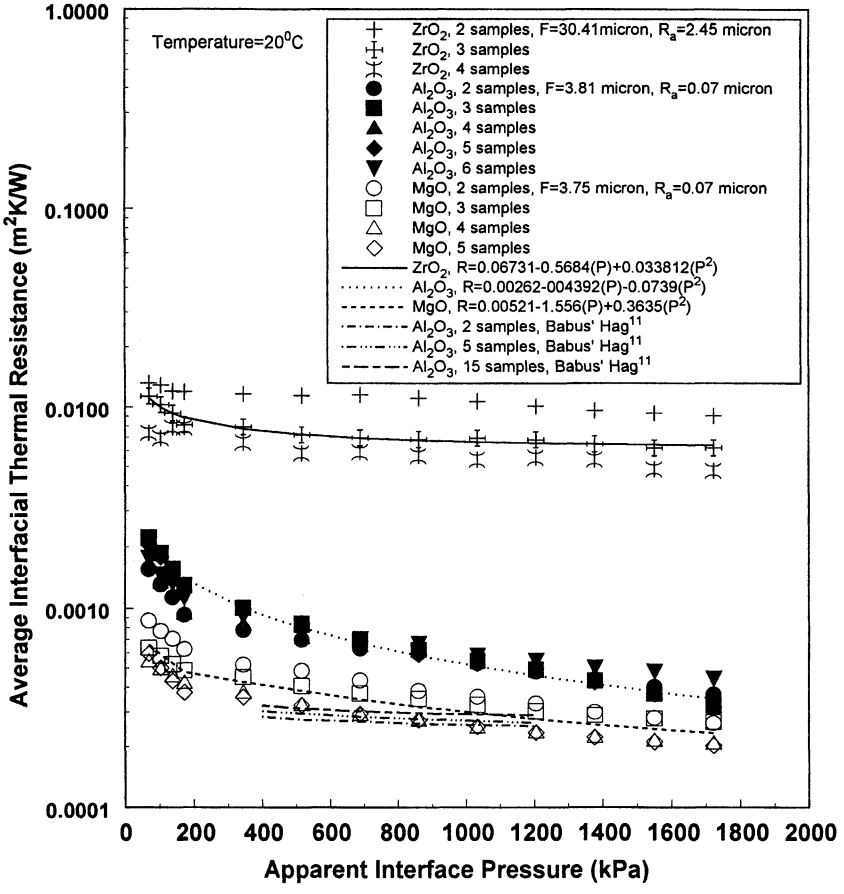

Fig. 5 Average interfacial thermal resistance between alumina, magnesia, and zirconia as a function of apparent interfacial pressure at 20°C.

creases less gradually with further increases in pressure. In the case of either two sapphire or magnesium-oxide samples constituting the stack, the total thermal resistance seems to be less dependent on applied pressure beyond 700 kPa. Figure 3 also indicates that the interfacial thermal resistance between the zirconia crystals is approximately twice that of the alumina and magnesia crystals. This may be attributed to the fact that the zirconia crystals were less flat and rougher than the single-crystal materials, consequently reducing the surface area for the effective flow of energy. Furthermore, because of the greater hardness of the zirconia crystals, the interfacial resistance between zirconia crystals appears to be less dependent on pressure when compared with alumina and magnesia crystals. Figure 3 also indicates the interfacial thermal resistance data of alumina samples (AOS Code 96R) as measured by Babus'Hag et al.[11] These resistance data are slightly lower than the present values for the same number of interfaces. Because of the small thickness of the samples, the buckle and waviness of the samples were pressed out with an increase in pressure, and hence, lowered the thermal resistance.

Figure 4 shows the total thermal contact resistance for both sapphire and magnesium-oxide crystals over the specified pressure range and at 60°C. Very similar trends are observed. Therefore, it appears that at these mean interface temperatures, the interfacial resistance is not significantly affected by the temperature.

Figure 5 indicates the average interfacial thermal resistance (total interfacial resistance divided by the number of crystal interfaces) as a function of interface pressure. As indicated in Table 2, the zirconia crystals are significantly less flat and more rough than the alumina and magnesia crystals. Consequently, the data indicated in Fig. 5 appear to fall into distinct groups. For the single-crystal materials (aluminum oxide and magnesium oxide), the average interfacial resistance values for stacks composed of several samples are much closer together than for the zirconia crystals that are relatively rougher and not as flat. Further, with an increase in pressure, the scatter in the experimental data was reduced, with the average value approaching a more uniform value. Figure 5 also presents a, best fit curve, which relates the average interfacial thermal resistance to the apparent interface pressure, for the different materials studied. For the sake of comparison, the thermal resistance per interface for alumina as measured by Babus'Hag et al.[11] has also been shown in Fig. 5.

A review of literature indicates that the interfacial thermal resistance is a function of the thickness of the crystal, applied interface pressure, absolute temperature of the crystal, and material properties (microhardness, thermal conductivity, and coefficient of linear expansion).[16–19] Among the surface characteristics, the most important parameters are the average surface roughness (R_a), and overall flatness (F), as indicated in Table 2. A parametric study of these variables suggest that the experimental data may be used to develop a correlation relating the dimensionless interfacial thermal resistance to the surface characteristics and material properties. The resulting expression is of the form

$$\frac{R_c k}{t} = 0.0003 \left[\left(\frac{R_a}{F}\right)\left(\frac{1}{\beta T}\right)\right]^3 \left(\frac{P}{H_v}\right)^{0.0167}$$

and the interfacial resistance may be written as

$$R_c = 0.0003 \left(\frac{t}{k}\right)\left[\left(\frac{R_a}{F}\right)\left(\frac{1}{\beta T}\right)\right]^3 \left(\frac{P}{H_v}\right)^{0.0167}$$

In the previously mentioned expression, the interfacial thermal resistance is nondimensionalized by the ratio of t/k, while the surafce characteristics are accounted for by the ratio of R_a/F. The term $1/\beta T$ accounts for the coefficient of thermal expansion of these materials as a function of temperature, and the apparent interface pressure has been nondimensionalized by the Vickers microhardness. The rationale for using these specific parameters (t/k, R_a/F, $1/\beta T$, and P/H_v) stems from the fact that these parameters predominantly influence the interfacial resistance.[20] Figure 6 compares the correlation that was developed for the interfacial thermal resistance in terms of dimensionless material properties, surface characteristics, apparent interface pressure, and mean interface temperature with the experimental date. As indicated by the equation, the ther-

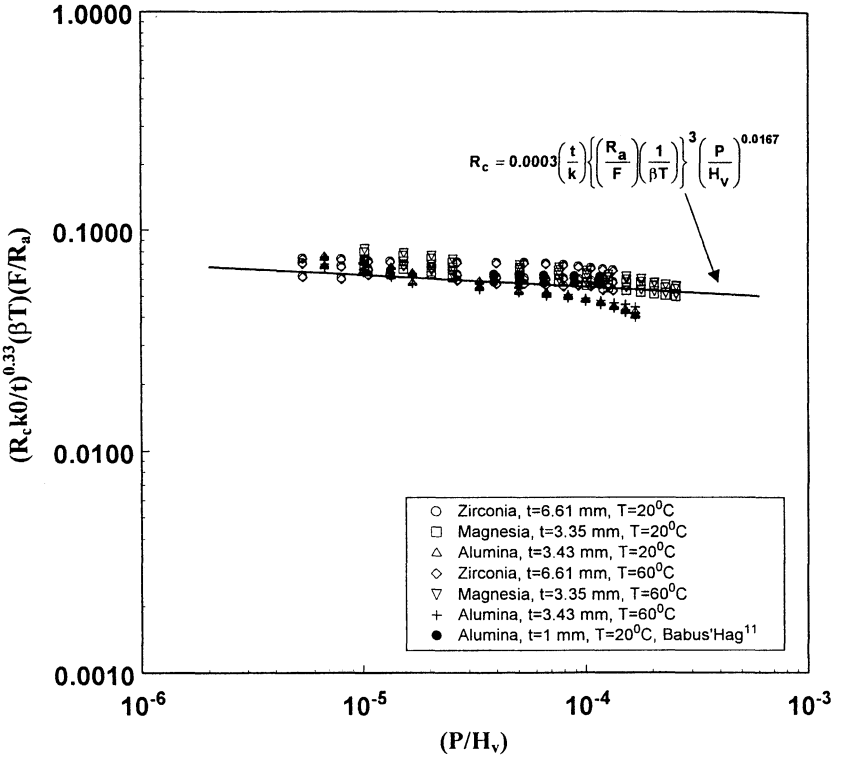

Fig. 6 Dimensionless average interfacial thermal resistance of alumina, magnesia, and zirconia at 20 and 60°C.

mal conductivity and surface characteristics play an important role. On the other hand, the apparent interface pressure does not appear to influence the interfacial thermal resistance significantly. This may be attributed to the fact that these materials possess extremely high microhardness values (Table 1), and hence, the actual contact area does not increase with an increase in pressure. At higher pressures, the data indicate a slight decreasing trend, this is possibly because of a slight reduction in the thickness of the crystals, thus enhancing the flow of energy. Furthermore, the thermal resistance per interface for alumina crystals as obtained by Babus'Hag et al.[11] has also been included. It is evident that the correlation fits their data accurately as well. This developed correlation may be used as a preliminary step toward the prediction of interfacial thermal resistance for the thermal design of solar concentrators.

Conclusions and Recommendations

An experimental investigation was conducted to determine the interfacial thermal resistance between multiple layers of single-crystal stacks of alumina and magnesia and yttrium-stabilized zirconia. The experiments were conducted over a range of apparent interface pressures of 70–1270 kPa and at mean interface temperatures of 20 and 60°C. The interfacial contact resistance decreased with an increase in apparent interface pressure, whereas the mean interface temperature did not significantly influence the experimental results.

These experimental data were used to develop a correlation for the interfacial thermal resistance. The resulting expression is presented as a function of dimensionless parameters for the ceramic crystal, including the material properties, surface characteristics, crystal thickness, apparent pressure, and interface temperature.

Considering the fact that these materials may be used as secondary concentrators, and consequently, might operate at significantly higher temperatures, it is recommended that an experimental investigation be conducted at actual operating temperatures. It is also recommended that the effect of surface characteristics be investigated more closely, and that other single-crystal materials be considered.

Acknowledgments

The authors are grateful to the Texas Engineering Experiment Station Center for Space Power and NASA Lewis Research Center for support of this investigation.

References

[1]Probert, S. D., and Jones, M. C., "Compressive Behaviour of Thin Layered Thermally Insulating Structural Supports," *Journal of Strain Analysis*, Vol. 1, No. 4, 1966, pp. 283–289.

[2]Probert, S. D., Thomas, T. R., and Warman, D., "A Mechanically Strong Thermal Insulator for Cryogenic Systems," *Thermal Insulation*, edited by S. D. Probert, and D. R. Hub, Elsevier, London, 1968, pp. 29–37.

[3]Mikesell, R. P., and Scott, R. B., "Heat Conduction Through Insulating Supports in Very Low Temperature Equipment," *Journal of Research of the National Bureau of Standards*, Vol. 57, No. 6, 1956, pp. 371–378.

[4]Fletcher, L. S., Blanchard, D. G., and Kinnear, K. P., "Thermal Conductance of Multilayered Metallic Sheets," AIAA Paper 91-1395, June 1991.

[5]Howells, R. I. L., Probert, S. D., and Jenkins, J. H., "Deformation of Stacks of Thin Layers Under Normal Compressive Loads," *Journal of Strain Analysis*, Vol. 4, No. 2, 1969, pp. 115–120.

[6]Chung, K. C., Benson, H. K., and Sheffield, J. W., "Thermal Contact Conductance of Ceramic Substrate Junctions," *Journal of Heat Transfer*, Vol. 117, May 1995, pp. 508–510.

[7]Fletcher, L. S., and Sparks, T. H., "Thermal Contact Conductance of Porous Ceramic Materials," *Proceedings of the NSF/DITAC Workshop on Thermal Conduction Enhancement in Microelectronics*, edited by A. Williams, Monash Univ., Melbourne, Australia, 1992, pp. 71–77.

[8]Thomas, T. R., and Probert, S. D., "Thermal Resistances of Some Multilayer Contacts Under Static Loads," *International Journal of Heat and Mass Transfer*, Vol. 9, Feb. 1966, pp. 739–754.

[9]Al-Astrabadi, F. R., O'Callaghan, P. W., Jones, A. M., and Probert, S. D., "Thermal Resistance Resulting from Commonly-Used Inserts Between Stainless-Steel, Static, Bearing Surfaces," *Wear*, Vol. 40, No. 3, 1976, pp. 339–350.

[10]Al-Astrabadi, F. R., Probert, S. D., O'Callaghan, P. W., and Jones, A. M., "Thermal Resistances of Stacks of Thin Layers Under Compression," *Journal of Mechanical Engineering Science*, Vol. 119, No. 4, pp. 167–174.

[11]Babus'Hag, R., Gibson, C., O'Callaghan, P. W., and Probert, S., "Multi-Layer Thermally-Insulating Ceramic Contact," AIAA Paper 89-0430, Jan. 1989.

[12]Schneider, S. J., *Engineered Metals Handbook—Ceramics and Glasses*, Vol. 4, ASM International, Washington, DC, 1991.

[13]Touloukian, Y. S., Powell, R. W., Ho, C. Y., and Klemens, P. G., *Thermophysical Properties of Matter-Thermal Conductivity*, Vol. 2, Plenum, New York, 1970.

[14]Kreith, F., *Fluid Flow Data Book*, Genium Publishing Corp., Schenectady, NY, 1984.

[15]Kline, S. J., and McClintock, F. A., "Describing Uncertainties in Single-Sample Experiments," *Mechanical Engineering*, Vol. 75, No. 1, 1953, pp. 1–8.

[16]Lambert, M. A., and Fletcher, L. S., "Metallic Coatings for Enhancement of Thermal Contact Conductance," *Journal of Thermophysics and Heat Transfer*, Vol. 8, No. 2, 1994, pp. 341–348.

[17]Lambert, M. A., and Fletcher, L. S., "Review of Thermal Contact Conductance of Metals," *Journal of Thermophysics and Heat Transfer*, Vol. 11, No. 2, 1994, pp. 129–140.

[18]McCool, J. I., "Comparison of Models for the Contact of Rough Surfaces," *Wear*, Vol. 107, No. 1, 1986, pp. 37–60.

[19]Yovanowich, M. M., "Thermal Contact Correlations," AIAA Paper 81-1164, June 1981.

[20]Sridhar, M., and Yovanovich, M., "Critical Review of Elastic and Plastic Thermal Contact Conductance Models and Comparison with Experiment," AIAA Paper 93-2776, July 1993.